



# Effect of immobilizing reagents on soil Cd and Pb lability under freeze-thaw cycles: Implications for sustainable agricultural management in seasonally frozen land



Renjie Hou<sup>a</sup>, Liuwei Wang<sup>a</sup>, David O'Connor<sup>a</sup>, Daniel C.W. Tsang<sup>b</sup>, Jörg Rinklebe<sup>c,d</sup>, Deyi Hou<sup>a,\*</sup>

<sup>a</sup> School of Environment, Tsinghua University, Beijing 100084, China

<sup>b</sup> Department of Civil and Environmental Engineering, The Hong Kong Polytechnic University, Hung Hom, Kowloon, Hong Kong, China

<sup>c</sup> University of Wuppertal, School of Architecture and Civil Engineering, Institute of Foundation Engineering, Water- and Waste-Management, Laboratory of Soil- and Groundwater-Management, Pauluskirchstraße 7, Wuppertal 42285, Germany

<sup>d</sup> Department of Environment, Energy and Geoinformatics, Sejong University, 98 Gunja-Dong, Seoul, Republic of Korea

## ARTICLE INFO

Handling Editor: Da Chen

### Keywords:

Soil remediation

Biochar

Bioavailability

Long-term effectiveness

## ABSTRACT

Agricultural soil contamination in seasonally frozen land threatens food security. It is necessary to investigate the effects of freeze-thaw cycles on heavy metal bioavailability so as to select suitable immobilization agents. In this study, the soil was collected from a mid-latitude agricultural site in Liaoning Province, China, which was spiked with cadmium ( $\text{Cd}^{2+}$ ) and lead ( $\text{Pb}^{2+}$ ). Four immobilization treatments were set up, including (i) corn stover biochar, (ii) organic fertilizer, (iii) combined biochar and organic fertilizer, and (iv) the control group. The immobilized soils were subjected to 16 freeze-thaw cycles to temperatures of  $-10\text{ }^{\circ}\text{C}$ ,  $-20\text{ }^{\circ}\text{C}$ , and  $-30\text{ }^{\circ}\text{C}$ . It was found that freeze-thaw cycling increased the labile cadmium (Cd) and lead (Pb) content in the soil (i.e., exchangeable). The organic fertilizer treatment performed best in short-term immobilization, which was demonstrated by the amount of diethylenetriaminepentaacetic acid (DTPA) extractable lead (Pb) being 17.3–53.3% lower than that of the other treatments, and 7.2–31.5% lower for cadmium (Cd). Biochar, on the other hand, displayed better long-term performance under freeze-thaw cycling. This is probably because the biochar's organic carbon content is relatively stable, and therefore, releases relatively little dissolved organic carbon (DOC) which could re-mobilize heavy metals. Furthermore, additional sorption sites are formed and the abundance of oxygen-containing functional groups increased when biochar breaks down during freeze-thaw cycles. Overall, the joint application of biochar and organic fertilizer had the greatest immobilization effect, which inhibited the cracking of soil aggregates, reduced the labile metal content, and displayed both short- and long-term immobilization effectiveness. It is suggested that combined biochar and organic fertilizer may offer an effective strategy for the sustainable agricultural management of cadmium (Cd) and lead (Pb) contaminated in seasonally frozen land.

## 1. Introduction

Degraded soils possess reduced capacity to perform a specified service, such as growing crops, thus hindering agricultural sustainability (Hou et al. 2020a). Soil degradation represents a global challenge (UNCCD, 2017), which has arisen due to factors such as soil erosion (Boardman et al., 2019; Liao et al., 2019; Patriche, 2019), acidification (Abd El-Halim and Omae, 2019; Tao et al., 2019), soil contamination (Hou, 2020; Wang et al., 2020e), compaction (Daraghmeh et al., 2019; Tassinari et al., 2019), and salinization (Narjary et al., 2019). Among these factors, soil contamination by

heavy metals, including cadmium (Cd) and lead (Pb), has received particular concern (Ma et al., 2019; O'Connor et al., 2019; Wang et al., 2020b). The is not only because of phytotoxicity associated with these heavy metals, but also because childhood Pb exposure is associated with life-long neurological disorders (NIOSH, 2016; O'Connor et al., 2020; Zhang et al., 2020a, 2019, 2020b) and Cd exposure can cause kidney damage and bone structure defects (Jia et al., 2020b; Wang et al., 2020c; WHO, 2017). Therefore, Cd and Pb in agricultural soil not only places a hurdle in the path to food security but can also affect food safety and human health (Deng and Li, 2016; Hou et al., 2020b; Zeb et al., 2020).

\* Corresponding author.

E-mail address: [houdedei@tsinghua.edu.cn](mailto:houdedei@tsinghua.edu.cn) (D. Hou).

<https://doi.org/10.1016/j.envint.2020.106040>

Received 7 May 2020; Received in revised form 19 July 2020; Accepted 3 August 2020

Available online 13 August 2020

0160-4120/ © 2020 The Author(s). Published by Elsevier Ltd. This is an open access article under the CC BY-NC-ND license

(<http://creativecommons.org/licenses/by-nc-nd/4.0/>).

Not all Cd and Pb contaminated soils pose significant risks to the environment and sustainable agriculture. It is widely acknowledged that the risk level directly relates to the bioavailability of contaminants, which is highly dependent on the local soil physicochemical properties and natural climate (Jia et al., 2020a; Wang et al., 2019a, 2019b). In particular, the risk of soil heavy metals relates to their geochemical fractionation (e.g., exchangeable, acid-soluble, reducible, oxidizable and residual) (Bashir et al., 2020; El-Naggar et al., 2018; Rinklebe and Shaheen, 2014; Rizwan et al., 2019; Salam et al., 2019; Shaheen et al., 2017). Risk mitigation strategies at heavy metal polluted sites, therefore, can rely on immobilization agents that cause a shift from the readily labile or potentially labile to non-labile form (Bolan et al., 2014; Salam et al., 2019; Wang et al., 2018). On the other hand, various environmental stresses may diminish heavy metal immobilization (Palansooriya et al., 2020a; Shen et al., 2019a; Yi et al., 2020; Zhao et al., 2020). For example, freeze-thaw aging destroys the soil structure, reduces the diameter of the soil particles and releases a large amount of dissolved organic matters that can re-mobilize soil metals, which in turn renders heavy metals more labile (Wei et al., 2018).

Farms that are located on mid-latitude seasonally frozen land, which includes the three major black soil zones, are crucial for meeting global food demand due to the characteristically high fertility of the soil (Hu et al., 2019). But these soils are also vulnerable to pollution stemming from anthropogenic activity, such as agricultural irrigation with contaminated water. During freeze-thaw processes, the expansion of ice leads to the breakdown of soil aggregates, which affects the physical and chemical properties of soil and promotes the release of dissolved organic carbon (DOC). In heavy metal contaminated soils, this DOC can act as a vector for plant uptake, thus increasing bioavailability and environmental risk (Araujo et al., 2019; Chen et al., 2018; Liu et al., 2018). Moreover, the breakdown of soil aggregates may also affect the soil's capacity to sorb heavy metals (Rui et al., 2019).

Recently, much research attention has been placed on biochar and organic fertilizers as immobilization agents for the remediation of heavy metal contaminated sites. Biochar is a carbon-rich material that can be yielded from various biomass feedstocks by burning them under oxygen-limited conditions (i.e., pyrolysis) (IBI, 2015; Wang et al., 2020d). Due to the well-developed pore structure, surface characteristics, and the alkaline mineral content of biochar (Bashagaluke et al., 2019; Jing et al., 2020; Palansooriya et al., 2020b; Wang et al., 2020a), this material can be applied to soil to immobilize heavy metals through various mechanisms, including cation- $\pi$  interactions, physisorption, surface precipitation, and liming effects (Hou, 2020; O'Connor et al., 2018; Shen et al., 2019b). Organic fertilizers, such as animal waste, plant residues and composts, are also rich in functional groups, such as carboxyl, hydroxyl and carbonyl, which can be also exploited to immobilize soil heavy metals via sorption processes (Lima et al., 2018; Montiel-Rozas et al., 2018). Moreover, organic fertilizers also typically poses high cation exchange capacity (CEC) which facilitates the removal of exchangeable heavy metals from soil (Guo et al., 2017; Liu et al., 2017).

However, little research has brought together the metal immobilizing performance of biochar or organic fertilizer amendments and the dynamics of seasonally frozen land. Previous studies of this environment have mainly focused on specific factors. For instance, Xu et al. (2018) reported that freeze-thaw cycles favored Cd immobilization within biochar amended soils due to enhanced surface complexation. A recent study by Meng et al. (2020) reported that the exchangeable fraction of Cd decreased with increasing numbers of the freeze-thaw cycles. But both of these studies lack an exploration of soil aggregate stability. Furthermore, the effectiveness of biochar-organic fertilizer co-application under freeze-thaw cycles need to be validated. This study comprehensively considers the above influencing factors, and is commenced to provide a proof-of-concept on biochar-assisted metal stabilization under freeze-thaw cycling.

The main objectives of this study were to identify: (1) the stability of

soil aggregates; (2) changes in metal geochemical fractions; and (3) the metal immobilization performance of corn stover biochar, organic fertilizer and combined amendments in soils subjected to freeze-thaw cycles. The result of this study may reveal the long-term stabilization mechanisms of immobilizing agents on soil Cd and Pb and provide fresh insights into the sustainable agricultural management in cold region.

## 2. Materials and methods

### 2.1. Materials

Agricultural soil was collected from the tillage layer (0–20 cm depth) of a typical agricultural site in the Hunhe river basin, Liaoning Province, China. Located in the mid-latitude, the sampled area is characterized by a seasonal freeze-thaw cycle. After removing plant roots and coarse gravel, the soil was spiked using  $\text{Pb}(\text{NO}_3)_2$  and Cd ( $\text{NO}_3)_2$  solution to simulate heavy metal contamination as per Shen et al. (2016). Briefly, 1 L of 125 mg/L  $\text{Pb}^{2+}$  and 450 mg/L  $\text{Cd}^{2+}$  solution was added per kg of soil, before being allowed to equilibrate for 28 d ( $20 \pm 2$  °C, 70% water holding capacity, stirring regularly) and then air-dried and sieved ( $< 2$  mm).

Considering the need for nutrient element replenishment and green sustainable restoration in farmland soil production, biochar and organic fertilizer were selected as soil amendments. Corn stover biochar was produced by pyrolysis at a highest treatment temperature of 500 °C for 2 h following an initial heating rate of 15 °C  $\text{min}^{-1}$  (Jinhefu Agricultural Technology Co., Ltd., China). The organic fertilizer was composed of a mixture of plant debris (85%), sheep manure (10%) and a compound microbial agent (5%) including bacteria, fungi and actinomycetes (Aijia Biotechnology Co., Ltd, China).

The pH value of the immobilization agents and the soil were measured in slurries with solid-to-liquid ratios of 1:20 and 1:5, respectively, using a pH meter (PHS-2F, Lichen Technology Co., Ltd, China) (IBI, 2015; ISO, 2005; Liu et al., 2018). Grain sizes were analyzed with a laser particle size analyzer (Winner 2308, Winner particle Co., Ltd, China). Cation exchange capacity (CEC) was measured by the ammonium acetate method (Wu et al., 2016). Organic carbon levels were determined using the potassium dichromate external heating method (Qian et al., 2013). Electrical conductivity (EC) was measured by conductivity meter (DDS-307A, INESA Scientific Instrument Co., Ltd, China). The elemental compositions were measured using an elemental analyzer (EA 2400 II, PerkinElmer Co., Ltd, USA). Soil was digested using  $\text{HNO}_3$ -HCl-HF (Nemati et al., 2010) before analyzing metal concentrations by ICP-OES (iCAP 7000, Thermo Fisher Scientific Co., Ltd, UK). The measured physicochemical properties of the soil and amendments are shown in Table 1.

### 2.2. Soil amendment and incubation

To extricate research results from the complex environment of seasonally frozen soils, amendment dosage rates were set at high, yet realistic, levels. Four treatments were prepared as follows: (i) control (soil without amendment), (ii) biochar (5% biochar and 95% soil dry wt.), (iii) organic fertilizer (5% organic fertilizer and 95% soil dry wt.), and (iv) combined biochar and organic fertilizer (2.5% biochar, 2.5% organic fertilizer, and 95% soil dry wt.). All treatments were conducted in triplicates. Each of the four treatments were manually homogenized before deionized water was added to achieve a soil moisture content of 30% wt., which lies between liquid and plastic limits of the soil. The four treatments were then incubated under constant temperature ( $25 \pm 2$  °C) for 28 days before the freeze-thaw cycling process commenced.

### 2.3. Freeze-thaw cycles

The four treatments were subjected to a modified freeze-thaw aging

**Table 1**  
Physicochemical properties of the soil and amendment materials.

Properties	Media		
	Soil	Biochar	Organic fertilizer
Grain size < 0.002 mm	23.5	-	-
0.002–0.02 mm	46.2	-	-
> 0.02 mm	31.3	-	-
CEC (cmol·kg <sup>-1</sup> )	9.73	55.15	39.54
pH	7.48	9.27	6.56
Organic carbon content (g·kg <sup>-1</sup> )	25.41	394.37	327.69
EC (ms·cm <sup>-1</sup> )	0.69	1.79	4.07
P content (g·kg <sup>-1</sup> )	0.9	2.3	25.8
H content (g·kg <sup>-1</sup> )	26.9	41.2	35.3
O content (g·kg <sup>-1</sup> )	341.6	396.9	461.7
Total Fe (g·kg <sup>-1</sup> )	23.65	2.37	9.78
Total Mn (mg·kg <sup>-1</sup> )	896.34	189.34	518.56
Total Al (mg·kg <sup>-1</sup> )	1879.45	510.45	1374.35
Total Cd (mg·kg <sup>-1</sup> )	126.65	-	-
Total Pb (mg·kg <sup>-1</sup> )	458.27	-	-

Note: - none detect.

method as per Hou et al. (2019). This method simulates the aging process of soils under different freezing temperatures and can effectively reveal the impact on long-term metal mobility. The freeze-thaw cycles were conducted in a temperature-controlled refrigerator (BC/BD-302SFA, Aucma Co., Ltd, China). The soil treatments were placed in aluminum boxes covered with polyethylene plastic film to maintain the soil moisture content. Three freezing temperatures (-10, -20 and -30 °C) were applied. In each freeze-thaw cycle, the four treatments were first frozen for 48 h. After that, the frozen treatments were thawed at 20 °C for 48 h. A total of 16 cycles were conducted (hereinafter referred as F1 – F16).

#### 2.4. Sample analysis

The effects of freeze-thaw cycles on biochar particle morphology were investigated by Field-Emission Scanning Electron Microscopy (FESEM) (Merlin, Zeiss Co., Ltd, Germany). In addition, changes to the biochar surface functional groups were analyzed using Fourier Transform Infrared Spectroscopy (FTIR) (IRTracer-100, Shimadzu Co., Ltd, Japan) with the wavenumber range of 4000 cm<sup>-1</sup> to 400 cm<sup>-1</sup> (resolution 4 cm<sup>-1</sup>).

To examine the effect of freeze-thaw aging on soil aggregate stability, water-stable soil aggregates were classified using the wet sieving method, that is, the soil was sieved and weighed (Elliott, 1986). The weight of a sample used for each test was 50 g (also conducted in triplicates). The water-stable aggregates were divided into five categories: (i) very large (> 2 mm), (ii) large (2–0.5 mm), (iii) medium (0.5–0.25 mm), (iv) fine (0.25–0.106 mm) and (v) silt & clay (< 0.106 mm). Several indicators were also determined to describe stable aggregate characteristics, including the mean weight diameter (MWD, mm), geometric mean diameter (GMD, mm), fractal dimension (D), the content of water-stable aggregates that are larger than 0.25 mm (WR<sub>0.25</sub>, wt%), and the percentage of aggregate destroyed (PAD, wt%) (Li et al., 2018; Zhao et al., 2018). The formulae used to calculate these indicators are provided in the supporting information.

To investigate changes in geochemical fractions, a five-step sequential extraction method was adopted (Tessier et al., 1979), which involved determining the (i) exchangeable (EXC), (ii) acid-soluble (e.g., bound to carbonates) (Carb), (iii) reducible (e.g., bound to Fe-Mn oxides) (Fe-Mn), (iv) oxidizable (e.g., bound to organic matter) (OM), and (v) residual (RES) fractions. In order to clearly reveal the effect of freeze-thaw aging and restorative materials on the transformation of geochemical fractions of heavy metals, the metal forms were divided into three pools: (1) the exchangeable fraction was defined as readily labile pool; (2) acid-soluble, reducible and oxidizable fractions were

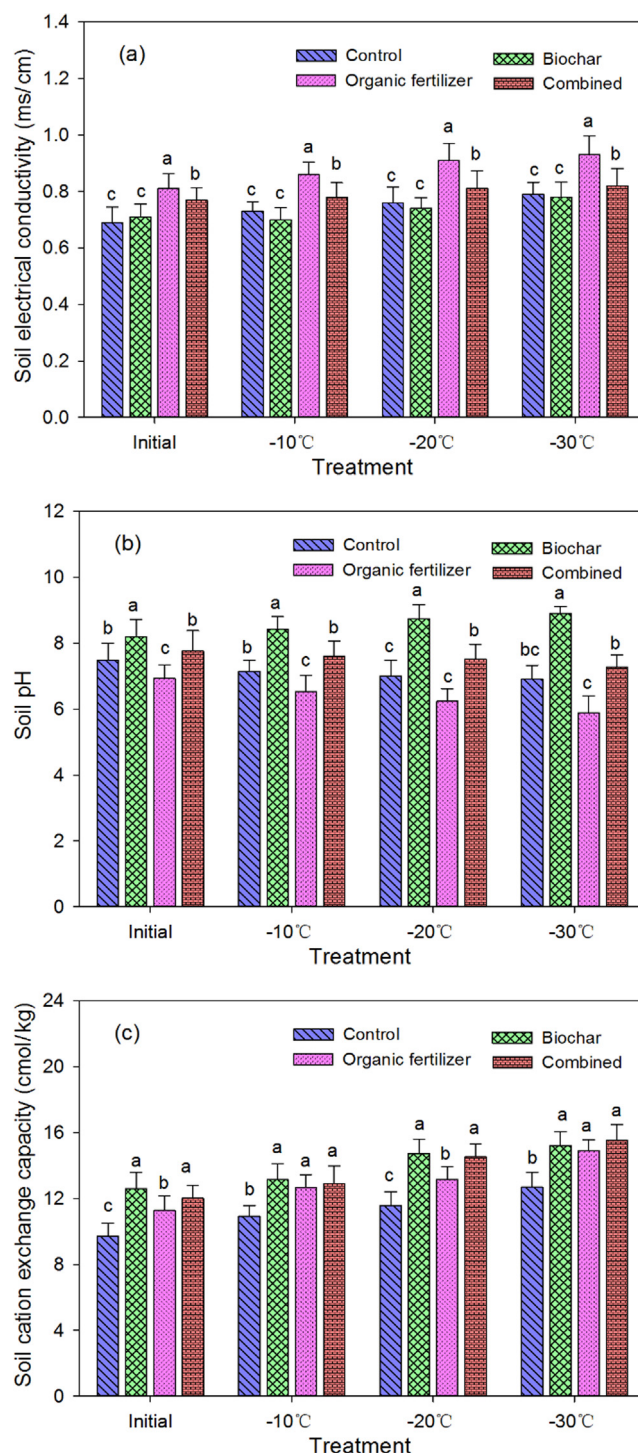


**Fig. 1.** Variation characteristics of soil parameters. (a) Soil EC for treatments frozen at different temperatures (-10 ~ -30 °C); (b) soil pH for treatments frozen at different temperatures (-10 ~ -30 °C); (c) soil CEC for treatments frozen at different temperatures (-10 ~ -30 °C).

defined as potentially labile pool and (3) the residual fraction was defined as non-labile pool. Additionally, approximations of Cd and Pb bioavailability were made by soil extraction with diethylenetriaminepentaacetic acid (DTPA) solution (US EPA, 2012). In addition, the dissolved organic carbon (DOC) content of the treatments were measured with a total organic carbon (TOC) analyzer (TOC-V WP, Shimadzu Co., Ltd, Japan) after extraction and centrifugation (Yoshida et al., 2018).

## 2.5. Statistical analysis

Statistical analysis was conducted using IBM SPSS 19.0. Differences in various treatments were analyzed using one-way analysis of variance (ANOVA) (Duncan's multiple range test).

## 3. Results and discussion

### 3.1. Soil EC, pH and CEC

The soil EC, pH and CEC under the four treatments are shown in Fig. 1. First of all, with the application of immobilization agents, the soluble salt segregants in the soil increased, and the conductivity of the soil solution also enhanced. Among the four treatments, the organic fertilizer treatment had the strongest effect, and its EC value was increased by 17.39%, 14.08% and 5.17%, compared to control, biochar and combined treatments, respectively. It is worth noting that in freeze–thaw aging, the soil EC values showed a certain increasing trend. For instance, at  $-10\text{ }^{\circ}\text{C}$  freezing temperature, the soil EC value increased by 5.79% compared to the initial unfrozen soil in the control treatment. In addition, with the decrease of freezing temperature, the EC value of soil gradually increased. It may be that freeze–thaw aging results in the cracking of soil particles and the release of soluble organic carbon and nitrogen, which in turn lead to an increase in the concentration of solutes in the soil solution (Juan et al., 2019). Besides, the organic fertilizer is rich in calcium (Ca), phosphorus (P), potassium (K) and other mineral elements, which increases the risk of soluble salt ion release under freeze–thaw aging (Parihar et al., 2020). Therefore, the EC value of soil under organic fertilizer treatment under freeze–thaw aging increased relative to the control group. For the biochar and combined treatments, biochar fixed the solute released by soil cracking via adsorption to a certain extent, thereby inhibiting the increase of soil electrical conductivity.

For soil pH, it can be found that for the initial unfrozen period, the application of organic fertilizer lowered the pH of the soil, while biochar caused it to increase. The organic fertilizer contains ammonium sulfate, superphosphate and other salts, and hydrolysis produces a certain amount of  $\text{H}^+$ , which causes the pH of the soil to decrease (Xu et al., 2020). However, the alkaline nature of biochar increases the pH of the soil (Wan et al., 2020). In addition, the freeze–thaw aging promoted the hydrolysis of salt segregants in the organic fertilizer treatment, and as the freezing temperature decreased, the range of soil pH changes increased. On the contrary, the soil pH value in biochar treatment increased under freeze–thaw aging.

Similarly, the addition of immobilization agents enhanced the adsorption ability of the soil colloid to cations, and the soil CEC under the organic fertilizer, biochar and combined treatments were increased by 29.29%, 15.82% and 21.46%, respectively, relative to the control group. In addition, for the control group, the soil CEC under freeze–thaw cycles with  $-10\text{ }^{\circ}\text{C}$  increased by 12.67% relative to the initial unfrozen soil. This is because the effect of frost heaving cracks large aggregates, increases the specific surface area of soil particles, provides more ion adsorption sites, and enhances the cation exchange capacity (Amin, 2020). With the decrease of freezing temperature, the increase range was significant.

### 3.2. Soil aggregates

The measured distribution of water-stable aggregates among the four treatments are shown in Fig. 2. It is noticeable that larger size aggregates proportionally increased after the addition of biochar or organic fertilizer to the soil. For instance, the fraction of very large aggregates in the unfrozen control soil was 0.143, which increased by 20.3%, 48.9% and 30.6% for the biochar, organic fertilizer and combined treatments, respectively. Large and medium sized aggregates also increased. An increase in soil aggregate size following soil amendment

was likely linked to the increased soil organic matter content, which is known to enhance soil aggregate stability (Eden et al., 2011). In addition, DOM may sorb to the well-developed carbon structure of biochar, which can also lead to increased stability of soil aggregates (Dong et al., 2016; Grunwald et al., 2017).

It was discovered that freeze–thaw cycling caused the breakdown of some soil aggregates. After 16 freeze–thaw cycles at a freezing temperature of  $-10\text{ }^{\circ}\text{C}$ , the fraction of very large aggregates in the control treatment reduced to 0.102. Meanwhile, the proportion of fine aggregates and silt and clay increased. It was also found that greater breakdown of aggregates occurred at lower freezing temperatures. For instance, the fraction of very large aggregates in the control treatment was 0.087 when the freezing temperature was  $-20\text{ }^{\circ}\text{C}$ , and 0.074 when exposed to  $-30\text{ }^{\circ}\text{C}$ . Meanwhile, the fractions of silt and clay increased by 9.3% and 12.1% at these temperatures, respectively. This is because the decrease of freezing temperature led to the increase of the expansion of ice in the soil, thus enhancing the extrusion strength of soil particles (Shen et al., 2020). This is consistent with the findings of Wei et al. (2018), who reported that soil cohesion gradually decreases with increased freezing strength.

Applications of biochar or organic fertilizer protected the treated soil from freeze–thaw induced aggregate breakdown to some extent. Although the proportion of large aggregates still decreased, the effect of freeze–thaw on the aggregate breakdown was diminished. For instance, when exposed to  $-10\text{ }^{\circ}\text{C}$  freezing, the very large aggregate fractions for the biochar, organic fertilizer and combined treatments were 15.5%, 27.6%, and 39.1% higher than that of the control treatment, respectively. This effect for the biochar treatment was probably due to its strong adsorption capacity, which increased cohesion between soil particles and inhibiting aggregate breakdown (Zhao et al., 2018). Furthermore, biochar was rich in organic matter. Particles released by aggregate breakdown can possibly combine with organic amendments through sorption processes to form medium-sized aggregates (Hagner et al., 2016). Compared to the control treatment, the proportion of medium sized aggregates in the biochar treatment was 24.7–53.6% higher, and for the organic fertilizer treatment it was 32.7–49.1% higher, but the greatest increase was found for the combined treatment, at 41.5–64.5% higher.

Generally, measured MWD parameters for the various treatments decreased with lower freezing temperature or increasing number of freeze–thaw cycles (Table 2). The amendments somewhat lessened the reduction of the MWD parameter, which was more obvious for the combined treatment. For instance, when the freeze temperature was  $-10\text{ }^{\circ}\text{C}$ , the MWD value was 0.79 mm under the control treatment, and the MWD values for the biochar, organic fertilizer and combined treatments were 0.08, 0.13 and 0.16 mm greater than that of the control treatment. A similar trend was observed for GMW and  $\text{WR}_{0.25}$ . Overall, the soil MWD, GWD, and  $\text{WR}_{0.25}$  values suggest that the soil aggregates were larger and more stable (Wang et al., 2015) in treatments with amendments applied.

The D value reflects the homogeneity of soil aggregates, with smaller D values being associated with more uniform (homogeneous) distributions of soil aggregates (Maggi, 2015). We discovered that the freeze–thaw process tended to increase the heterogeneity of the aggregates, showing larger D values. The combined treatment helped preserve the uniformity of the aggregate distribution. Moreover, under different freezing scenarios, the PAD values for the biochar, organic fertilizer and combined treatments decreased compared to the control treatment. Dai et al. (2019) suggested that the application of organic amendments increases soil macromolecular organic components, such as cellulose and polysaccharides, which help maintain the uniformity and stability of soil aggregates. Ojeda et al. (2015) reported that the porous and granular structure of biochar promoted the formation of stable composites in soil, and that organic matter attached to biochar enhanced the polymerization effect.

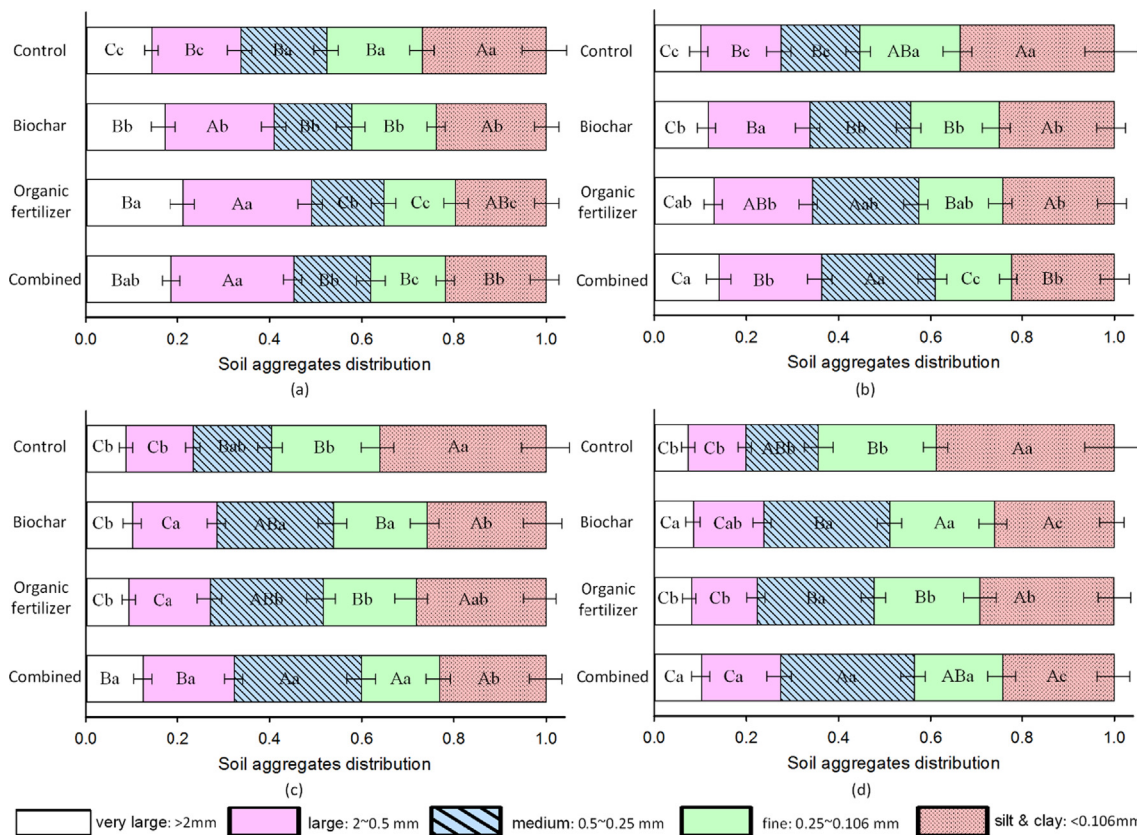


**Fig. 2.** Distribution of soil water-stable aggregates. (a) Unfrozen soil, (b) after 16 freeze–thaw cycles at  $-10\text{ }^{\circ}\text{C}$ , (c) after 16 freeze–thaw cycles at  $-20\text{ }^{\circ}\text{C}$ , (d) after 16 freeze–thaw cycles at  $-30\text{ }^{\circ}\text{C}$ . Note: different capital letters indicate significant differences of five soil water-stable aggregate fractions ( $p < 0.05$ ); different lower case letters indicate significant differences of soil water stable-aggregates under different treatments ( $p < 0.05$ ).

### 3.3. Geochemical fractions

The addition of the biochar or organic fertilizer was observed to reduce the readily labile pool of both Cd and Pb in the unfrozen soil (Fig. 3). For Cd, the readily labile pools were reduced by 21.6%, 31.2% and 25.1% by the biochar, organic fertilizer and combined treatments,

respectively, in comparison with the control treatment. Further analysis showed that the potentially labile pool was the highest in organic fertilizer treatment, which increased by 19.02% relative to the control treatment. The non-labile pools in biochar and combined treatments were increased by 33.46% and 43.88%, respectively, relative to the control group. It showed that the readily labile pool decreased by

**Table 2**  
Characteristics of soil aggregates.

Freezing temperature	Treatments	MWD (mm)	GMD (mm)	PAD (%)	D	WR <sub>0.25</sub> (%)
$-10\text{ }^{\circ}\text{C}$	Control	$0.79 \pm 0.11\text{bcd}$	$0.23 \pm 0.03\text{bc}$	$64.79 \pm 4.23\text{abcd}$	$2.6989 \pm 0.012\text{ ns}$	$41.85 \pm 3.11\text{abcd}$
	Biochar	$0.87 \pm 0.08\text{abc}$	$0.25 \pm 0.01\text{abc}$	$59.41 \pm 5.11\text{ cd}$	$2.6912 \pm 0.021$	$44.21 \pm 2.19\text{abc}$
	Organic Fertilizer	$0.92 \pm 0.13\text{ab}$	$0.27 \pm 0.04\text{ab}$	$57.56 \pm 6.23\text{d}$	$2.6851 \pm 0.008$	$47.37 \pm 1.79\text{a}$
	Combined	$0.95 \pm 0.15\text{a}$	$0.28 \pm 0.05\text{a}$	$54.68 \pm 4.54\text{d}$	$2.6754 \pm 0.017$	$49.65 \pm 2.23\text{a}$
$-20\text{ }^{\circ}\text{C}$	Control	$0.71 \pm 0.07\text{ cd}$	$0.19 \pm 0.00\text{c}$	$69.53 \pm 3.22\text{abc}$	$2.7083 \pm 0.022$	$39.25 \pm 2.03\text{bcd}$
	Biochar	$0.82 \pm 0.06\text{abcd}$	$0.24 \pm 0.03\text{bc}$	$63.51 \pm 3.79\text{abcd}$	$2.6852 \pm 0.014$	$42.18 \pm 1.78\text{abcd}$
	Organic Fertilizer	$0.84 \pm 0.09\text{abc}$	$0.25 \pm 0.05\text{abc}$	$62.76 \pm 4.13\text{bcd}$	$2.6844 \pm 0.019$	$43.67 \pm 2.04\text{abc}$
	Combined	$0.90 \pm 0.08\text{abc}$	$0.27 \pm 0.02\text{ab}$	$58.96 \pm 2.87\text{ cd}$	$2.6791 \pm 0.009$	$46.35 \pm 1.96\text{ab}$
$-30\text{ }^{\circ}\text{C}$	Control	$0.68 \pm 0.05\text{d}$	$0.17 \pm 0.03\text{c}$	$74.23 \pm 3.54\text{a}$	$2.7174 \pm 0.014$	$36.51 \pm 2.23\text{d}$
	Biochar	$0.79 \pm 0.04\text{bcd}$	$0.23 \pm 0.03\text{bc}$	$72.48 \pm 4.27\text{ab}$	$2.6965 \pm 0.017$	$41.67 \pm 4.31\text{abcd}$
	Organic Fertilizer	$0.71 \pm 0.10\text{ cd}$	$0.19 \pm 0.04\text{c}$	$69.59 \pm 3.65\text{abc}$	$2.7046 \pm 0.023$	$38.75 \pm 2.52\text{ cd}$
	Combined	$0.86 \pm 0.07\text{abc}$	$0.25 \pm 0.00\text{abc}$	$61.42 \pm 2.78\text{bcd}$	$2.6892 \pm 0.015$	$44.41 \pm 1.51\text{abc}$
<i>Average values</i>						
$-10\text{ }^{\circ}\text{C}$		$0.88 \pm 0.12\text{a}$	$0.26 \pm 0.03\text{a}$	$59.11 \pm 2.11\text{b}$	$2.6877 \pm 0.008\text{ ns}$	$45.77 \pm 1.12\text{a}$
$-20\text{ }^{\circ}\text{C}$		$0.82 \pm 0.09\text{b}$	$0.24 \pm 0.02\text{b}$	$63.69 \pm 1.79\text{b}$	$2.6893 \pm 0.005$	$42.86 \pm 1.49\text{b}$
$-30\text{ }^{\circ}\text{C}$		$0.76 \pm 0.05\text{c}$	$0.21 \pm 0.02\text{c}$	$69.43 \pm 1.54\text{a}$	$2.7020 \pm 0.009$	$40.33 \pm 0.87\text{c}$
	Control	$0.73 \pm 0.08\text{c}$	$0.20 \pm 0.01\text{c}$	$69.52 \pm 2.23\text{a}$	$2.7082 \pm 0.002\text{ ns}$	$39.20 \pm 0.92\text{c}$
	Biochar	$0.83 \pm 0.05\text{b}$	$0.23 \pm 0.00\text{b}$	$65.13 \pm 2.46\text{b}$	$2.6910 \pm 0.006$	$42.69 \pm 1.33\text{bc}$
	Organic Fertilizer	$0.82 \pm 0.09\text{b}$	$0.24 \pm 0.01\text{b}$	$63.30 \pm 2.97\text{c}$	$2.6914 \pm 0.005$	$43.26 \pm 1.45\text{b}$
	Combined	$0.91 \pm 0.11\text{a}$	$0.27 \pm 0.02\text{a}$	$58.35 \pm 1.89\text{bc}$	$2.6812 \pm 0.002$	$46.80 \pm 1.39\text{a}$

Note: Different lower-case letters indicate significant differences of soil water-stable aggregates indicators ( $p < 0.05$ ), while ns means that there are no significant differences ( $p > 0.05$ ).

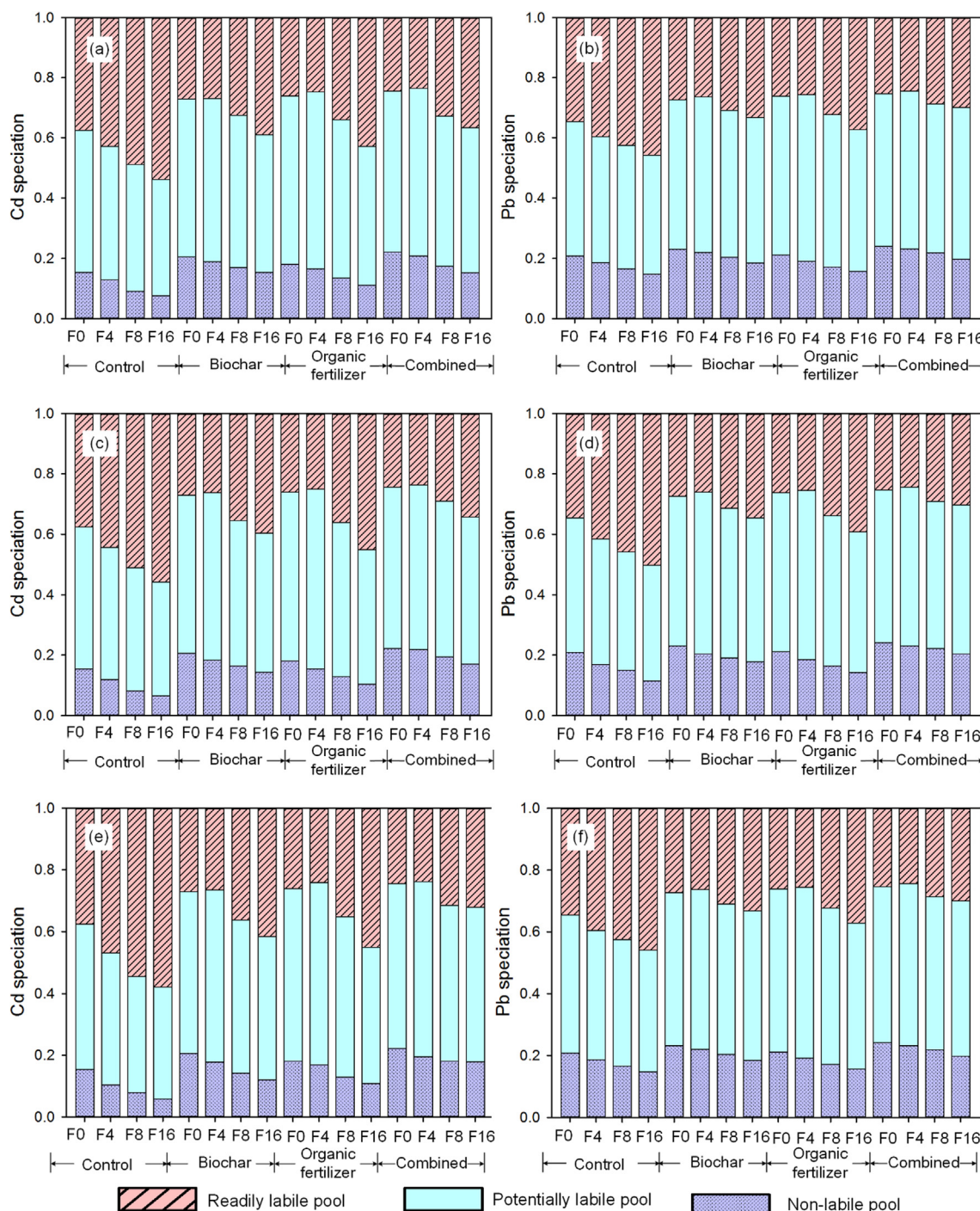


**Fig. 3.** Geochemical fractions of Cd and Pb under different treatments across 16 freeze–thaw cycles (F0–F16). (a) Cd speciation for treatments frozen at  $-10^{\circ}\text{C}$ , (b) Pb speciation for treatments frozen at  $-10^{\circ}\text{C}$ , (c) Cd speciation for treatments frozen at  $-20^{\circ}\text{C}$ , (d) Pb speciation for treatments frozen at  $-20^{\circ}\text{C}$ , (e) Cd speciation for treatments frozen at  $-30^{\circ}\text{C}$ , and (f) Pb speciation for treatments frozen at  $-30^{\circ}\text{C}$ .

organic fertilizer treatment was mainly transformed into potentially labile pool, and they are mainly converted into non-labile pools in the biochar and combined treatments. For Pb, the trend was consistent with that of Cd.

Organic fertilizer contains humus and other macromolecular organic substances that immobilize Cd and Pb through surface complexation and cation- $\pi$  interactions (Qi et al., 2016; Shi et al., 2016). Anions, such as  $\text{S}^{2-}$  and  $\text{PO}_4^{3-}$  in organic amendment materials may also form stable heavy metal precipitates, resulting in a shift of oxidizable metals to the residual fraction (Egene et al., 2018). In addition, oxygen-containing functional groups on the surface of biochar (Section 3.5) can

bind with Cd and Pb. As a carbon-rich material, biochar tends to render metals less labile in terms of the operational definition of metal fractionation (Qian et al., 2019). A certain amount of Fe–Mn oxides may also derive during the production and natural aging of biochar, which would also bind with heavy metals (Lin et al., 2017). Moreover, the alkaline mineral content of biochar increases the metal immobilization through precipitation reactions or electrostatic interactions due to more negatively charged surfaces (Bolan et al., 2014; Kumar et al., 2018; O'Connor et al., 2018).

Overall, the proportion of readily labile pool of Pb was less than that of Cd, indicating that Pb was less mobile (Ahmadipour et al., 2014;

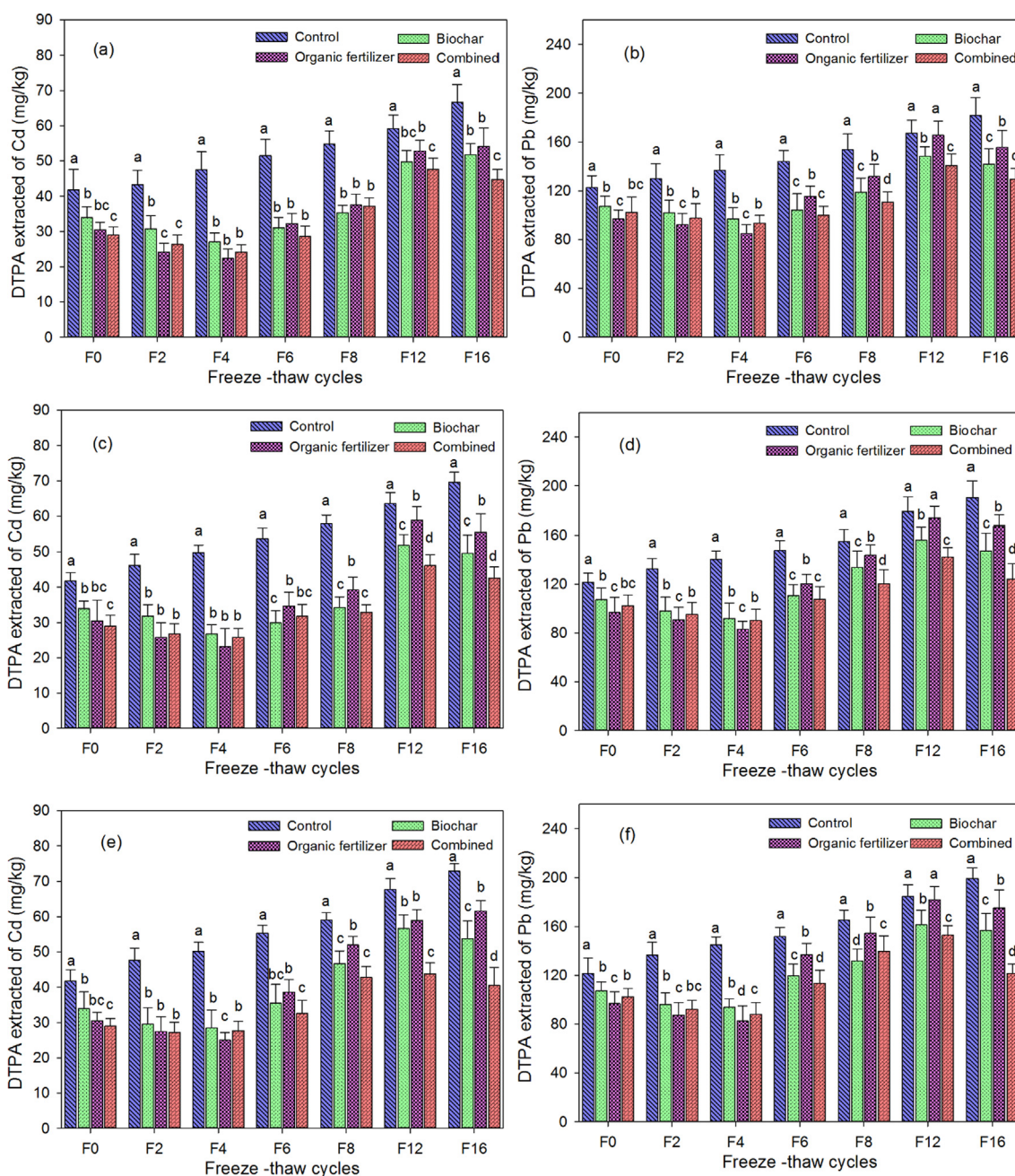


**Fig. 4.** DTPA extraction as an approximation of the bioavailability of Cd and Pb in different treatments across 16 freeze–thaw cycles (F0–F16). (a) Cd extracted from treatments frozen at  $-10^{\circ}\text{C}$ , (b) Pb extracted from treatments frozen at  $-10^{\circ}\text{C}$ , (c) Cd extracted from treatments frozen at  $-20^{\circ}\text{C}$ , (d) Pb extracted from treatments frozen at  $-20^{\circ}\text{C}$ , (e) Cd extracted from treatments frozen at  $-30^{\circ}\text{C}$ , and (f) Pb extracted from treatments frozen at  $-30^{\circ}\text{C}$  Note: Different lower case letters indicate significant differences between treatments ( $P < 0.05$ ).

Kede et al., 2014; Rinklebe and Shaheen, 2014, 2017; Salam et al., 2019; Shaheen et al., 2017; Wieczorek et al., 2018). The first-order hydrolysis constant for ions determines the complexation capacity of functional groups of biochar and organic matters for metal ions, and the complexation effect decreases with the increase of the first-order hydrolysis constant negative logarithm  $\text{p}K_1$  ( $\text{Pb}$  (7.8) >  $\text{Cd}$  (10.1)), thus Pb would theoretically bind more strongly (Ahmadipour et al., 2014; Wieczorek et al., 2018).

The breakdown of soil aggregates during the freeze–thaw process (Section 3.2) may have facilitated an increase in labile heavy metals (Islam et al., 2017) by releasing dissolved organic carbon (DOC), which renders metals more mobile (Li et al., 2016). With increasing number of freeze–thaw cycles, the readily labile pools of Cd and Pb tended to

increase gradually, and the potentially labile and non-labile pools decreased gradually. For instance, when a freezing temperature of  $-10^{\circ}\text{C}$  was applied, the readily labile pools of Cd and Pb in the control treatment increased by 43.5% and 36.8%, respectively, compared to the unfrozen group. Simultaneously, the potentially labile pools of Cd and Pb in the control treatment decreased by 17.89% and 13.52%, respectively. In addition, the non-labile pool of metal also showed a decreasing trend. Lower freezing temperatures aggravated this effect. When the freezing temperature was  $-30^{\circ}\text{C}$ , the readily labile pools of Cd and Pb increased by 54.4% and 46.9%, respectively, compared to the unfrozen group.

Moreover, the readily labile pools of Cd and Pb under the biochar and organic fertilizer treatments decreased after four freeze–thaw

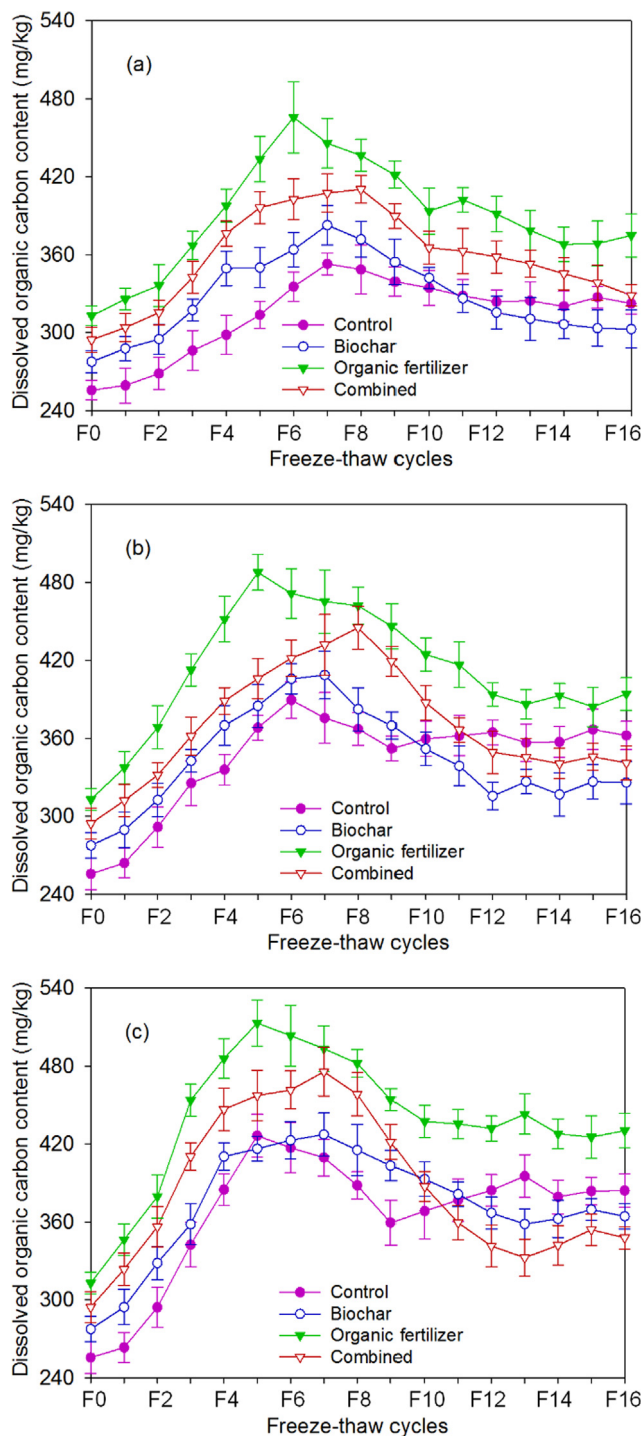


**Fig. 5.** Effects of freeze–thaw cycles (F1–16) on the dissolved organic carbon content. Note: a, b, c represent the freezing temperature of  $-10$ ,  $-20$  and  $-30$  °C, respectively.

cycles and then increased with further cycles. When the freezing temperature was  $-10$  °C, the readily labile pools of Cd under the organic fertilizer and biochar treatments decreased by 20.4% and 27.67%, respectively, compared with the control treatment. Meanwhile, the non-labile pools increased by 35.43% and 65.14%, respectively. It is noteworthy that the efficiency of the organic fertilizer treatment was lower than that of biochar in the context of freeze–thaw cycling. Although the initial freeze–thaw cycle produces a large number of macromolecular organic substances that bind with metals through complexation (Shi and Schulin, 2018), DOC would also be released as the number of

freeze–thaw cycles increased, which increases the mobilization potential for heavy metals.

Contrary to the reducing efficiency of the organic fertilizer treatment, the effectiveness of the biochar treatment increased with freeze–thaw cycling. Biochar particle cracking and mild oxidation caused by freeze–thaw cycles may have increased its specific surface area and its abundance of oxygen-containing functional groups (Section 3.5) (Hale et al., 2012). It is notable that the combined application of biochar and organic fertilizer performed better than both amendments applied alone, apparently gaining both the short- and long-term treatment benefits of the organic fertilizer and biochar treatments, respectively.

### 3.4. Bioavailability

The DTPA extractable Cd and Pb content in the soil, which was used as an approximation for their bioavailability, decreased significantly after the addition of the amendments (Fig. 4). One-way analysis of variance (ANOVA) ( $p < 0.05$ ) was used to analyze the significant differences of the DTPA extractable metal under different treatments in each period. For unfrozen treatments, the DTPA extraction of Cd for the biochar, organic fertilizer, and combined treatments decreased by 18.9%, 26.3%, and 31.3%, respectively, compared to the control treatment, whilst for Pb it decreased by 12.6%, 21.1% and 16.4%, respectively.

The amount of Cd and Pb extracted by DTPA increased with increasing freeze–thaw cycles. When comparing the control treatment after 16 freeze–thaw cycles at  $-10$  °C to before freezing, for instance, the amount of Cd and Pb extracted was 59.6% and 48.3% higher, respectively. Nevertheless, the amount of metals extracted from the organic fertilizer, biochar and combined treatments first decreased and then increased as the number of freeze–thaw cycles increased further. For instance, after 6 freeze–thaw cycles at  $-10$  °C, the DTPA extractable Cd and Pb content decreased by 24.2% and 15.8%, respectively, compared to the unfrozen organic fertilizer treatment. However, by the time the number of freeze–thaw cycles had reached 16, the DTPA extractable Cd and Pb content was 61.3% and 53.1% higher than that of the unfrozen organic fertilizer treatment, respectively.

For the biochar treatment and the combined treatment, DTPA extraction of heavy metals decreased by different degrees compared with organic fertilizer treatment after successive freeze–thaw cycles. This is because in the initial freeze–thaw cycles, the breakdown of soil aggregates promoted rapid complexation of macromolecular organic matter and heavy metals carried by organic fertilizer (Manasypov et al., 2015). However, successive freeze–thaw cycling accelerated oxidative decomposition of macro-sized organic matter, thus reducing the stability of metal–organic complexes (Yi et al., 2015). On the contrary, the adsorption capacity of biochar may have increased as successive freeze–thaw cycles broke down its structure. In addition, an increased abundance of oxygen-containing functional groups on the biochar would have promoted further surface complexation reactions.

### 3.5. Amendment decomposition

Decomposition of the organic fertilizer and biochar materials during freeze–thaw cycling can significantly reduce their immobilization effectiveness because of DOC release. For the non-frozen treatments (F0), both biochar and organic fertilizer increased the DOC content (Fig. 5). With increasing number of freeze–thaw cycles (F1–16), the DOC content increased first and then decreased. This is probably because the freeze–thaw process reduced the stability of soil aggregates which lead to the release of DOC (Watanabe et al., 2019). Meanwhile, the freeze–thaw cycles cause microorganism lysis and death, thus releasing small molecules of sugar and amino acids, thus also increasing DOC release (Song et al., 2017). After multiple freeze–thaw cycles, the DOC released by the soil aggregates would gradually decrease (Fuss et al.,



**Table 3**  
Pearson correlation coefficients between metal liability and dissolved organic carbon.

Freezing temperature	Geochemical fractions	Cd				Pb			
		Control	Biochar	Organic fertilizer	Combined	Control	Biochar	Organic fertilizer	Combined
−10°C	Readily labile	0.694*	0.551*	0.567*	0.516	0.771*	0.685*	0.595	0.547
	Potentially labile	0.522	0.459	0.564*	0.487*	0.487	0.512	0.619*	0.507
	Non-labile	−0.392	−0.473*	−0.473	−0.549*	−0.383	−0.461*	−0.439	−0.518*
−20°C	Readily labile	0.737**	0.656*	0.693	0.567	0.651*	0.512	0.573*	0.549
	Potentially labile	0.507	0.571	0.621*	0.549	0.419	0.509	0.481*	0.425*
	Non-labile	−0.328	−0.507*	−0.393	−0.468*	−0.371	−0.495*	−0.397	−0.518*
−30°C	Readily labile	0.712*	0.535	0.624*	0.592	0.673*	0.512*	0.567*	0.584
	Potentially labile	0.461	0.478*	0.557*	0.512*	0.476	0.425	0.481*	0.542*
	Non-labile	−0.371	−0.497*	−0.427	−0.469*	−0.491	−0.389*	−0.482	−0.545*

Note: “\*\*\*” represents that the correlation passes the significance test of  $p < 0.01$ ; “\*\*” represents that the correlation passes the significance test of  $p < 0.05$ .



**Fig. 6.** Morphology of biochar samples at different freezing temperatures (a represents the unfrozen sample; b, c, d represent the freezing temperature of −10, −20 and −30 °C, respectively).

2016). It is noteworthy that some microorganisms have resistance towards freezing forces. These organisms may play a vital role in the mineralization and decomposition of soil DOC, accompanied by the generation of CO<sub>2</sub> and water (Walz et al., 2017). In addition, as the freezing temperature decreased, the maximum value of soil DOC under various treatments showed an increasing trend.

The content of soil DOC determines the metal forms to a certain extent, and the Pearson correlation coefficients between metal liability and DOC were explored (Table 3). It can be seen that the readily labile forms of Cd and Pb had a positive correlation with DOC, but the application of immobilization agents diminished this trend. It may be that biochar reduces the production of soil DOC, and organic fertilizer complexes with some labile forms of Cd and Pb, thus reducing the correlation between them (Guo et al., 2020; Rajapaksha et al., 2018). Simultaneously, the potentially labile forms of metal also had a positive correlation with DOC, but the correlation was weaker than the readily

labile ones. In addition, the non-labile forms of Cd and Pb showed a negative correlation with DOC, and the negative correlation was significantly enhanced under biochar and combined treatments, which also confirmed the passivation effect of biochar and combined remediation on metals.

We found that the morphology of the biochar amendment changed under different freezing conditions (Fig. 6). The cell structure of the feedstock remained visible before freezing (F0), with the biochar displaying a smooth surface and uniform and clear the pores (Fig. 6a). Successive freeze–thaw cycles caused damage to the cell structure and caused cracks to form. This may have increased the available sites for adsorption, and may also favor internal oxidation of biochar (Dong et al., 2017). In addition, the surface of biochar became much rougher with more cracks appeared with lower freezing temperatures, indicating the breakdown of biochar during the aging process (Fig. 6 bcd).

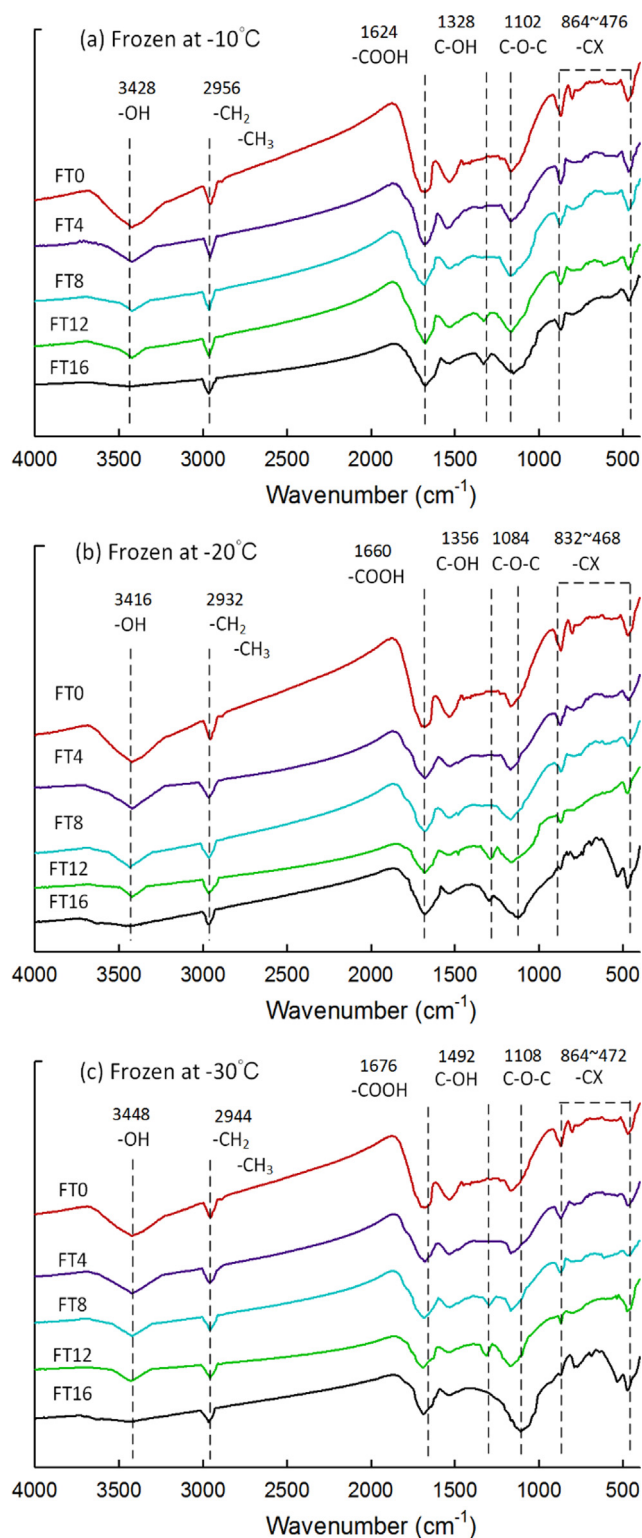


Fig. 7. FTIR spectra of biochar under different freezing temperatures (a, b, c represent the freezing temperature of  $-10$ ,  $-20$  and  $-30$  °C, respectively).

The observed biochar FTIR spectra demonstrates that there were differences in the abundance of functional groups before and after the biochar treatment was subjected to freeze–thaw cycling (Fig. 7). A band was identified at  $3428\text{ cm}^{-1}$ , which represents the  $\text{-OH}$  stretching vibration. The band at  $2956\text{ cm}^{-1}$  reveals the asymmetric C–H stretching vibration, indicating aliphatic groups. The band at  $1624\text{ cm}^{-1}$  is the stretching vibration of  $\text{-COOH}$ . At  $1328$  and

$1102\text{ cm}^{-1}$ , the stretching vibration of C–OH of the alcohol and carboxylic acid groups overlapped with the stretching vibration of C–O–C of the ester and ether groups. In addition, the  $476\text{--}864\text{ cm}^{-1}$  absorption peak represents the stretching vibration of  $\text{-CX}$  of aromatic compounds (Wu et al., 2018). When the freezing temperature was  $-10$  °C, the intensity of the absorption peak at  $3428\text{ cm}^{-1}$  decreased with increasing freeze–thaw cycles, indicating that repeated freeze–thawing diminishes the abundance of  $\text{-OH}$  functional groups on the surface of biochar. On the contrary, the amplitude and width of the absorption peak in  $1624$ ,  $1328$  and  $1102\text{ cm}^{-1}$  showed an increasing trend, indicating that the number of  $\text{-COOH}$ , C–O–C and C–OH functional groups on the biochar surface increased. This might be because microorganisms in the soil environment accelerated the oxidation of organic carbon, resulting in an increase in oxygen-containing functional groups (Heitkötter and Marschner, 2015). As the freezing temperature decreased, the width and amplitude of the  $\text{-COOH}$ , C–O–C, and C–OH stretching vibration peaks also increased.

Overall, the biochar amendment was found to have several advantages in the freeze–thaw environment, including, (1) the organic carbon content of biochar is recalcitrant, thus it releases DOC relatively slowly (Fig. 5); (2) the breakdown of biochar’s matrix structure may enhance its sorption capacity towards Cd and Pb as well as DOC (Fig. 6); (3) the number of oxygen-containing functional groups increased after freeze–thaw cycling, which would favor surface complexation between heavy metals and the biochar (Fig. 7). Therefore, it can be reasoned that corn-stover biochar has beneficial characteristics for the long-term immobilization of heavy metals in seasonally frozen land.

#### 4. Conclusions

We found that freeze–thaw cycles damages soil aggregates, while the application of biochar and organic fertilizer hindered this effect through the formation of medium-sized aggregates. Freeze–thaw cycling increased the exchangeable fractions of Pb and Cd in the soil, which is likely related to the observed release of DOC and breakdown of soil aggregates. The immobilization agents selected for this study have shown to be effective at mitigating metal leaching potential through surface complexation and other interactions. Compared with organic fertilizer, biochar is more stable and associated with less DOC release. Furthermore, biochar breakdown during freeze–thaw cycles creates sorption sites and increases the abundance of oxygen-containing functional groups which immobilize heavy metals. While biochar rendered good long-term immobilization performance, the organic fertilizer displayed better Cd and Pb stabilization in the short-term by causing a greater to stable geochemical fractionations. The combined biochar and organic fertilizer treatment, not only reduced the potential for DOC release, but also improved in physicochemical properties during freeze–thaw cycling (e.g., increase oxygen-containing functional groups for surface complexation). It is, therefore, concluded that combined treatments may immobilize Cd and Pb contaminants effectively. These findings provide a proof-of-concept for the efficient management of contaminated soils in locations of seasonally frozen land. What’s more, the optimal mixing ratio of biochar and organic fertilizer is worthy of in-depth exploration, and the results from the laboratory needs to be further verified in field.

#### CRedit authorship contribution statement

**Renjie Hou:** Investigation, Methodology, Writing - original draft. **Liuwei Wang:** Investigation, Writing - original draft. **David O’Connor:** Writing - review & editing. **Daniel C.W. Tsang:** Writing - review & editing. **Jörg Rinklebe:** Writing - review & editing. **Deyi Hou:** Conceptualization, Resources, Supervision, Writing - review & editing.

## Declaration of Competing Interest

The authors declare that they have no known competing financial interests or personal relationships that could have appeared to influence the work reported in this paper.

## Acknowledgements

This work was supported by National Key Research and Development Program of China (Grant No. 2018YFC1801300).

## Appendix A. Supplementary material

Supplementary data to this article can be found online at <https://doi.org/10.1016/j.envint.2020.106040>.

## References

- Abd El-Halim, A., Omae, H., 2019. Performance assessment of nanoparticulate lime to accelerate the downward movement of calcium in acid soil. *Soil Use Manage.* 35, 683–690.
- Ahmadipour, F., Bahramifar, N., Ghasempouri, S.M., 2014. Fractionation and mobility of cadmium and lead in soils of amol area in Iran, using the modified BCR sequential extraction method. *Chem. Speciation Bioavailab.* 26, 31–36.
- Amin, A., 2020. Carbon sequestration, kinetics of ammonia volatilization and nutrient availability in alkaline sandy soil as a function on applying calotropis biochar produced at different pyrolysis temperatures. *Sci. Total Environ.* 726, 138489.
- Araujo, E., Strawn, D.G., Morra, M., Moore, A., Ferraciu Alleoni, L.R., 2019. Association between extracted copper and dissolved organic matter in dairy-manure amended soils. *Environ. Pollut.* 246, 1020–1026.
- Bashagaluke, J.B., Logah, V., Opoku, A., Tuffour, H.O., Sarkodie-Addo, J., Quansah, C., 2019. Soil loss and run-off characteristics under different soil amendments and cropping systems in the semi-deciduous forest zone of Ghana. *Soil Use Manage.* 35, 617–629.
- Bashir, A., Rizwan, M., Zia Ur Rehman, M., Zubair, M., Riaz, M., Qayyum, M.F., Alharby, H.F., Bamagoos, A.A., Ali, S., 2020. Application of co-composted farm manure and biochar increased the wheat growth and decreased cadmium accumulation in plants under different water regimes. *Chemosphere* 246: 125809.
- Boardman, J., Vandaele, K., Evans, R., Foster, I.D., 2019. Off-site impacts of soil erosion and runoff: Why connectivity is more important than erosion rates. *Soil Use Manage.* 35, 245–256.
- Bolan, N., Kunhikrishnan, A., Thangarajan, R., Kumpiene, J., Park, J., Makino, T., Kirkham, M.B., Scheckel, K., 2014. Remediation of heavy metal(loid)s contaminated soils – To mobilize or to immobilize? *J. Hazard. Mater.* 266, 141–166.
- Chen, Y., Shi, J., Tian, X., Jia, Z., Wang, S., Chen, J., Zhu, W., 2018. Impact of dissolved organic matter on Zn extractability and transfer in calcareous soil with maize straw amendment. *J. Soils Sediments* 19, 774–784.
- Dai, H., Chen, Y., Liu, K., Li, Z., Qian, X., Zang, H., Yang, X., Zhao, Y., Shen, Y., Li, Z., Sui, P., 2019. Water-stable aggregates and carbon accumulation in barren sandy soil depend on organic amendment method: A three-year field study. *J. Cleaner Prod.* 212, 393–400.
- Daraghme, O.A., Petersen, C.T., Munkholm, L.J., Znova, L., Obour, P.B., Nielsen, S.K., Green, O., 2019. Impact of tillage intensity on clay loam soil structure. *Soil Use Manage.* 35, 388–399.
- Deng, X., Li, Z., 2016. Economics of Land Degradation in China. In: Nkonya, E., Mirzabaev, A., von Braun, J. (Eds.), *Economics of Land Degradation and Improvement – A Global Assessment for Sustainable Development*. Springer International Publishing, Cham.
- Dong, X., Guan, T., Li, G., Lin, Q., Zhao, X., 2016. Long-term effects of biochar amount on the content and composition of organic matter in soil aggregates under field conditions. *J. Soils Sediments* 16, 1481–1497.
- Dong, X., Li, G., Lin, Q., Zhao, X., 2017. Quantity and quality changes of biochar aged for 5 years in soil under field conditions. *Catena* 159, 136–143.
- Eden, M., Schjønning, P., Moldrup, P., De Jonge, L.W., 2011. Compaction and rotovation effects on soil pore characteristics of a loamy sand soil with contrasting organic matter content. *Soil Use Manage.* 27, 340–349.
- Egene, C.E., Van Poucke, R., Ok, Y.S., Meers, E., Tack, F.M.G., 2018. Impact of organic amendments (biochar, compost and peat) on Cd and Zn mobility and solubility in contaminated soil of the Campine region after three years. *Sci. Total Environ.* 626, 195–202.
- El-Naggar, A., Shaheen, S.M., Ok, Y.S., Rinklebe, J., 2018. Biochar affects the dissolved and colloidal concentrations of Cd, Cu, Ni, and Zn and their phytoavailability and potential mobility in a mining soil under dynamic redox-conditions. *Sci. Total Environ.* 624, 1059–1071.
- Elliott, E., 1986. Aggregate structure and carbon, nitrogen, and phosphorus in native and cultivated soils 1. *Soil Sci. Soc. Am. J.* 50, 627–633.
- Fuss, C.B., Driscoll, C.T., Groffman, P.M., Campbell, J.L., Christenson, L.M., Fahey, T.J., Fisk, M.C., Mitchell, M.J., Templer, P.H., Durán, J., Morse, J.L., 2016. Nitrate and dissolved organic carbon mobilization in response to soil freezing variability. *Biogeochemistry* 131, 35–47.
- Grunwald, D., Kaiser, M., Junker, S., Marhan, S., Piepho, H.P., Poll, C., Bamminger, C., Ludwig, B., 2017. Influence of elevated soil temperature and biochar application on organic matter associated with aggregate-size and density fractions in an arable soil. *Agric. Ecosyst. Environ.* 241, 79–87.
- Guo, G., Lei, M., Chen, T., Yang, J., 2017. Evaluation of different amendments and foliar fertilizer for immobilization of heavy metals in contaminated soils. *J. Soils Sediments* 18, 239–247.
- Guo, X., Xie, X., Liu, Y., Wang, C., Yang, M., Huang, Y., 2020. Effects of digestate DOM on chemical behavior of soil heavy metals in an abandoned copper mining areas. *J. Hazard. Mater.* 393, 122436.
- Hagner, M., Kemppainen, R., Jauhiainen, L., Tiilikkala, K., Setälä, H., 2016. The effects of birch (*Betula* spp.) biochar and pyrolysis temperature on soil properties and plant growth. *Soil Tillage Res.* 163, 224–234.
- Hale, B., Evans, L., Lambert, R., 2012. Effects of cement or lime on Cd, Co, Cu, Ni, Pb, Sb and Zn mobility in field-contaminated and aged soils. *J. Hazard. Mater.* 199–200, 119–127.
- Heitkötter, J., Marschner, B., 2015. Interactive effects of biochar ageing in soils related to feedstock, pyrolysis temperature, and historic charcoal production. *Geoderma* 245–246, 56–64.
- Hou, D., 2020. *Sustainable Remediation of Contaminated Soil and Groundwater: Materials, Processes, and Assessment* ed's.
- Hou, D., Bolan, N.S., Tsang, D.C.W., Kirkham, M.B., O'Connor, D., 2020a. Sustainable soil use and management: an interdisciplinary and systematic approach. *Sci. Total Environ.*
- Hou, D., O'Connor, D., Igalavithana, A.D., Alessi, D.S., Luo, J., Tsang, D.C.W., Sparks, D.L., Yamauchi, Y., Rinklebe, J., Ok, Y.S., 2020b. Metal contamination and bioremediation of agricultural soils for food safety and sustainability. *Nat. Rev. Earth Environ.* 1, 366–381.
- Hou, R., Li, T., Fu, Q., Liu, D., Cui, S., Zhou, Z., Yan, P., Yan, J., 2019. Effect of snow-straw collocation on the complexity of soil water and heat variation in the Songnen Plain, China. *Catena* 172, 190–202.
- Hu, T., Zhao, T., Zhao, K., Shi, J., 2019. A continuous global record of near-surface soil freeze/thaw status from AMSR-E and AMSR2 data. *Int. J. Remote Sens.* 40, 6993–7016.
- IBI, 2015. *Standardized Product Definition and Product Testing Guidelines for Biochar That Is Used in Soil*. International Biochar Initiative.
- Islam, M.N., Taki, G., Nguyen, X.P., Jo, Y.-T., Kim, J., Park, J.-H., 2017. Heavy metal stabilization in contaminated soil by treatment with calcined cockle shell. *Environ. Sci. Pollut. Res.* 24, 7177–7183.
- ISO. ISO 10390-2005. *Soil Quality - Determination of pH*. International Organization for Standardization.
- Jia, H., Hou, D., O'Connor, D., Pan, S., Zhu, J., Bolan, N.S., Mulder, J., 2020. Exogenous phosphorus treatment facilitates chelation-mediated cadmium detoxification in perennial ryegrass (*Lolium perenne* L.). *J. Hazard. Mater.* 389, 121849.
- Jia, H., Hou, D., O'Connor, D., Pan, S., Zhu, J., Bolan, N.S., Mulder, J. Exogenous phosphorus treatment facilitates chelation-mediated cadmium detoxification in perennial ryegrass (*Lolium perenne* L.). *J. Hazard. Mater.* 389, 121849.
- Jing, F., Chen, X., Wen, X., Liu, W., Hu, S., Yang, Z., Guo, B., Luo, Y., Yu, Q., Xu, Y., 2020. Biochar effects on soil chemical properties and mobilization of cadmium (Cd) and lead (Pb) in paddy soil. *Soil Use Manage.* 36, 320–327.
- Juan, Y., Tian, L., Sun, W., Qiu, W., Curtin, D., Gong, L., Liu, Y., 2019. Simulation of soil freezing-thawing cycles under typical winter conditions: implications for nitrogen mineralization. *J. Soils Sediments* 20, 143–152.
- Kede, M.L., Correia, F.V., Conceição, P.F., Junior, S.F., Marques, M., Moreira, J.C., Pérez, D.V., 2014. Evaluation of mobility, bioavailability and toxicity of Pb and Cd in contaminated soil using TCLP, BCR and earthworms. *Int. J. Environ. Res. Public Health* 11, 11528–11540.
- Kumar, A., Joseph, S., Tschansky, L., Privat, K., Schreiter, I.J., Schüth, C., Graber, E.R., 2018. Biochar aging in contaminated soil promotes Zn immobilization due to changes in biochar surface structural and chemical properties. *Sci. Total Environ.* 626, 953–961.
- Li, H., Ye, X., Geng, Z., Zhou, H., Guo, X., Zhang, Y., Zhao, H., Wang, G., 2016. The influence of biochar type on long-term stabilization for Cd and Cu in contaminated paddy soils. *J. Hazard. Mater.* 304, 40–48.
- Li, R., Kan, S., Zhu, M., Chen, J., Ai, X., Chen, Z., Zhang, J., Ai, Y., 2018. Effect of different vegetation restoration types on fundamental parameters, structural characteristics and the soil quality index of artificial soil. *Soil Tillage Res.* 184, 11–23.
- Liao, K.W., Guo, J.J., Fan, J.C., Lee, C.C., Huang, C.L., 2019. Evaluation of rainfall kinetic energy and erosivity in northern Taiwan using kriging with climate characteristics. *Soil Use Manage.* 35, 630–642.
- Lima, J.Z., Raimondi, I.M., Schalch, V., Rodrigues, V.G.S., 2018. Assessment of the use of organic composts derived from municipal solid waste for the adsorption of Pb, Zn and Cd. *J. Environ. Manage.* 226, 386–399.
- Lin, L., Qiu, W., Wang, D., Huang, Q., Song, Z., Chau, H.W., 2017. Arsenic removal in aqueous solution by a novel Fe-Mn modified biochar composite: Characterization and mechanism. *Ecotoxicol. Environ. Saf.* 144, 514–521.
- Liu, H., Xu, F., Xie, Y., Wang, C., Zhang, A., Li, L., Xu, H., 2018. Effect of modified coconut shell biochar on availability of heavy metals and biochemical characteristics of soil in multiple heavy metals contaminated soil. *Sci. Total Environ.* 645, 702–709.
- Liu, Y.N., Guo, Z.H., Xiao, X.Y., Wang, S., Jiang, Z.C., Zeng, P., 2017. Phytostabilisation potential of giant reed for metals contaminated soil modified with complex organic fertilizer and fly ash: A field experiment. *Sci. Total Environ.* 576, 292–302.
- Ma, L., Abuduwaii, J., Li, Y., Liu, W., 2019. Anthropogenically disturbed potentially toxic elements in roadside topsoils of a suburban region of Bishkek, Central Asia. *Soil Use Manage.* 35, 283–292.
- Maggi, F., 2015. Experimental evidence of how the fractal structure controls the

- hydrodynamic resistance on granular aggregates moving through water. *J. Hydrol.* 528, 694–702.
- Manasyapov, R.M., Vorobyev, S.N., Loiko, S.V., Kritzkov, I.V., Shirokova, L.S., Shevchenko, V.P., Kirpotin, S.N., Kulizhsky, S.P., Kolesnichenko, L.G., Zemtsov, V.A., Sinkinov, V.V., Pokrovsky, O.S., 2015. Seasonal dynamics of organic carbon and metals in thermokarst lakes from the discontinuous permafrost zone of western Siberia. *Biogeosciences* 12, 3009–3028.
- Meng, Z., Huang, S., Xu, T., Deng, Y., Lin, Z., Wang, X., 2020. Transport and transformation of Cd between biochar and soil under combined dry-wet and freeze-thaw aging. *Environ. Pollut.* 263.
- Montiel-Rozas, M.M., Domínguez, M.T., Madejón, E., Madejón, P., Pastorelli, R., Renella, G., 2018. Long-term effects of organic amendments on bacterial and fungal communities in a degraded Mediterranean soil. *Geoderma* 332, 20–28.
- Narjary, B., Meena, M.D., Kumar, S., Kamra, S.K., Sharma, D.K., Triantafyllis, J., 2019. Digital mapping of soil salinity at various depths using an EM38. *Soil Use Manage.* 35, 232–244.
- Nemati, K., Abu Bakar, N.K., Bin Abas, M.R., Sobhanzadeh, E., Low, K.H., 2010. Comparative study on open system digestion and microwave assisted digestion methods for metal determination in shrimp sludge compost. *J. Hazard Mater.* 182, 453–459.
- NIOSH, 2016. NIOSH Pocket Guide to Chemical Hazards - Lead. National Institute for Occupational Safety Health.
- O'Connor, D., Hou, D.Y., Ok, Y.S., Mulder, J., Duan, L., Wu, Q.R., Wang, S.X., Tack, F.M.G., Rinklebe, J., 2019. Mercury speciation, transformation, and transportation in soils, atmospheric flux, and implications for risk management: A critical review. *Environ. Int.* 126, 747–761.
- O'Connor, D., Peng, T., Zhang, J., Tsang, D.C.W., Alessi, D.S., Shen, Z., Bolan, N.S., Hou, D., 2018. Biochar application for the remediation of heavy metal polluted land: A review of in situ field trials. *Sci. Total Environ.* 619–620, 815–826.
- O'Connor, D., Hou, D., Ok, Y.S., Lanphear, B.P., 2020. The effects of iniquitous lead exposure on health. *Nature Sustain* 3, 77–79.
- Ojeda, G., Mattana, S., Ávila, A., Alcañiz, J.M., Volkman, M., Bachmann, J., 2015. Are soil–water functions affected by biochar application? *Geoderma* 249–150, 1–11.
- Palansooriya, K.N., Shaheen, S.M., Chen, S.S., Tsang, D.C.W., Hashimoto, Y., Hou, D., Bolan, N.S., Rinklebe, J., Ok, Y.S., 2020. Soil amendments for immobilization of potentially toxic elements in contaminated soils: A critical review. *Environ. Int.* 134, 105046.
- Parihar, C.M., Singh, A.K., Jat, S.L., Dey, A., Nayak, H.S., Mandal, B.N., Saharawat, Y.S., Jat, M.L., Yadav, O.P., 2020. Soil quality and carbon sequestration under conservation agriculture with balanced nutrition in intensive cereal-based system. *Soil Tillage Res.* 202.
- Patriche, C.V., 2019. Quantitative assessment of rill and interrill soil erosion in Romania. *Soil Use Manage.* 35, 257–272.
- Qi, Y., Zhu, J., Fu, Q., Hu, H., Huang, Q., Violante, A., 2016. Sorption of Cu by organic matter from the decomposition of rice straw. *J. Soils Sediments* 16, 2203–2210.
- Qian, D., Fan, H., Zhou, L., Wu, M., Guo, P., 2013. Effects of Freeze-Thaw Cycles on Brown Forest Soil Available Phosphorus in Northeastern China. *Commun. Soil Sci. Plant Anal.* 44, 2361–2370.
- Qian, T.T., Wu, P., Qin, Q.Y., Huang, Y.N., Wang, Y.J., Zhou, D.M., 2019. Screening of wheat straw biochars for the remediation of soils polluted with Zn (II) and Cd (II). *J. Hazard. Mater.* 362, 311–317.
- Rajapaksha, A.U., Alam, M.S., Chen, N., Alessi, D.S., Igalavithana, A.D., Tsang, D.C.W., Ok, Y.S., 2018. Removal of hexavalent chromium in aqueous solutions using biochar: Chemical and spectroscopic investigations. *Sci. Total Environ.* 625, 1567–1573.
- Rinklebe, J., Shaheen, S.M., 2014. Assessing the Mobilization of Cadmium, Lead, and Nickel Using a Seven-Step Sequential Extraction Technique in Contaminated Floodplain Soil Profiles Along the Central Elbe River, Germany. *Water, Air, Soil Pollution* 225.
- Rinklebe, J., Shaheen, S.M., 2017. Geochemical distribution of Co, Cu, Ni, and Zn in soil profiles of Fluvisols, Luvisols, Gleysols, and Calcisols originating from Germany and Egypt. *Geoderma* 307, 122–138.
- Rizwan, M., Ali, S., Zia Ur Rehman, M., Adrees, M., Arshad, M., Qayyum, M.F., Ali, L., Hussain, A., Chatha, S.A.S., Imran, M., 2019. Alleviation of cadmium accumulation in maize (*Zea mays* L.) by foliar spray of zinc oxide nanoparticles and biochar to contaminated soil. *Environ. Pollut.* 248, 358–367.
- Rui, D., Wu, Z., Ji, M., Liu, J., Wang, S., Ito, Y., 2019. Remediation of Cd- and Pb-contaminated clay soils through combined freeze-thaw and soil washing. *J. Hazard Mater.* 369, 87–95.
- Salam, A., Shaheen, S.M., Bashir, S., Khan, I., Wang, J., Rinklebe, J., Rehman, F.U., Hu, H., 2019. Rice straw- and rapeseed residue-derived biochars affect the geochemical fractions and phytoavailability of Cu and Pb to maize in a contaminated soil under different moisture content. *J. Environ. Manage.* 237, 5–14.
- Shaheen, S.M., Kwon, E.E., Biswas, J.K., Tack, F.M.G., Ok, Y.S., Rinklebe, J., 2017. Arsenic, chromium, molybdenum, and selenium: Geochemical fractions and potential mobilization in riverine soil profiles originating from Germany and Egypt. *Chemosphere* 180, 553–563.
- Shen, Y., Tang, T., Zuo, R., Tian, Y., Zhang, Z., Wang, Y., 2020. The effect and parameter analysis of stress release holes on decreasing frost heaves in seasonal frost areas. *Cold Reg. Sci. Technol.* 169.
- Shen, Z., McMillan, O., Jin, F., Al-Talabaa, A., 2016. Salisbury biochar did not affect the mobility or speciation of lead in kaolin in a short-term laboratory study. *J. Hazard. Mater.* 316, 214–220.
- Shen, Z., Pan, S., Hou, D., O'Connor, D., Jin, F., Mo, L., Xu, D., Zhang, Z., Alessi, D.S., 2019a. Temporal effect of MgO reactivity on the stabilization of lead contaminated soil. *Environ. Int.* 131.
- Shen, Z.T., Fan, X.L., Hou, D.Y., Jin, F., O'Connor, D., Tsang, D.C.W., Ok, Y.S., Alessi, D.S., 2019b. Risk evaluation of biochars produced from Cd-contaminated rice straw and optimization of its production for Cd removal. *Chemosphere* 233, 149–156.
- Shi, P., Schulin, R., 2018. Erosion-induced losses of carbon, nitrogen, phosphorus and heavy metals from agricultural soils of contrasting organic matter management. *Sci. Total Environ.* 618, 210–218.
- Shi, Z., Wang, P., Peng, L., Lin, Z., Dang, Z., 2016. Kinetics of heavy metal dissociation from natural organic matter: roles of the carboxylic and phenolic sites. *Environ. Sci. Technol.* 50, 10476–10484.
- Song, Y., Zou, Y., Wang, G., Yu, X., 2017. Altered soil carbon and nitrogen cycles due to the freeze-thaw effect: A meta-analysis. *Soil Biol. Biochem.* 109, 35–49.
- Tao, H., Pan, W.L., Carter, P., Wang, K., 2019. Addition of lignin to lime materials for expedited pH increase and improved vertical mobility of lime in no-till soils. *Soil Use Manage.* 35, 314–322.
- Tassinari, D., Andrade, M.I.d.C., Dias Junior, M.d.S., Martins, R.P., Rocha, W.W., Pais, P. S.A.M., de Souza, Z.R., 2019. Soil compaction caused by harvesting, skidding and wood processing in eucalyptus forests on coarse-textured tropical soils. *Soil Use Manage.* 35, 400–411.
- Tessier, A., Campbell, P.G., Bisson, M., 1979. Sequential extraction procedure for the speciation of particulate trace metals. *Anal. Chem.* 51, 844–851.
- UNCCD, 2017. Global land outlook.
- US EPA, 2012. Standard operating procedure for an in vitro bioaccessibility assay for lead in soil. United States Environmental Protection Agency.
- Walz, J., Knoblauch, C., Böhme, L., Pfeiffer, E.-M., 2017. Regulation of soil organic matter decomposition in permafrost-affected Siberian tundra soils - Impact of oxygen availability, freezing and thawing, temperature, and labile organic matter. *Soil Biol. Biochem.* 110, 34–43.
- Wan, Z., Sun, Y., Tsang, D.C.W., Xu, Z., Khan, E., Liu, S.-H., Cao, X., 2020. Sustainable impact of tartaric acid as electron shuttle on hierarchical iron-incorporated biochar. *Chem. Eng. J.* 395.
- Wang, L., Bolan, N.S., Tsang, D.C.W., Hou, D., 2020a. Green immobilization of toxic metals using alkaline enhanced rice husk biochar: Effects of pyrolysis temperature and KOH concentration. *Sci. Total Environ.* 720, 137584.
- Wang, L., Chen, L., Tsang, D.C.W., Kua, H.W., Yang, J., Ok, Y.S., Ding, S., Hou, D., Poon, C.S., 2019a. The roles of biochar as green admixture for sediment-based construction products. *Cem. Concr. Compos.* 104.
- Wang, L., Cho, D.W., Tsang, D.C.W., Cao, X., Hou, D., Shen, Z., Alessi, D.S., Ok, Y.S., Poon, C.S., 2019b. Green remediation of As and Pb contaminated soil using cement-free clay-based stabilization/solidification. *Environ. Int.* 126, 336–345.
- Wang, L., Hou, D., Cao, Y., Ok, Y.S., Tack, F.M.G., Rinklebe, J., O'Connor, D., 2020b. Remediation of mercury contaminated soil, water, and air: A review of emerging materials and innovative technologies. *Environ. Int.* 134.
- Wang, L., Li, X., Tsang, D.C.W., Jin, F., Hou, D., 2020c. Green remediation of Cd and Hg contaminated soil using humic acid modified montmorillonite: Immobilization performance under accelerated ageing conditions. *J. Hazard. Mater.* 387, 122005.
- Wang, L., Ok, Y.S., Tsang, D.C., Alessi, D.S., Rinklebe, J., Wang, H., Mašek, O., Hou, R., O'Connor, D., Hou, D., 2020. New trends in biochar pyrolysis and modification strategies: feedstock, pyrolysis conditions, sustainability concerns and implications for soil amendment. *Soil Use Manage.*
- Wang, L., Wu, W.-M., Bolan, N.S., Tsang, D.C.W., Li, Y., Qin, M., Hou, D., 2020e. Environmental fate, toxicity and risk management strategies of nanoplastics in the environment: Current status and future perspectives. *J. Hazard. Mater.*
- Wang, L., Yu, K.Q., Li, J.S., Tsang, D.C.W., Poon, C.S., Yoo, J.C., Baek, K., Ding, S.M., Hou, D.Y., Dai, J.G., 2018. Low-carbon and low-alkalinity stabilization/solidification of high-Pb contaminated soil. *Chem. Eng. J.* 351, 418–427.
- Wang, Y., Zhang, J.H., Zhang, Z.H., 2015. Influences of intensive tillage on water-stable aggregate distribution on a steep hillslope. *Soil Tillage Res.* 151, 82–92.
- Watanabe, T., Tateno, R., Imada, S., Fukuzawa, K., Isobe, K., Urakawa, R., Oda, T., Hosokawa, N., Sasai, T., Inagaki, Y., Hishi, T., Toda, H., Shibata, H., 2019. The effect of a freeze-thaw cycle on dissolved nitrogen dynamics and its relation to dissolved organic matter and soil microbial biomass in the soil of a northern hardwood forest. *Biogeochemistry* 142, 319–338.
- Wei, X., Huang, C., Wei, N., Zhao, H., He, Y., Wu, X., 2018. The impact of freeze-thaw cycles and soil moisture content at freezing on runoff and soil loss. *Land Degrad. Dev.*
- WHO, 2017. Ten chemicals of major health concern. World Health Organization.
- Wieczorek, J., Baran, A., Urbański, K., Mazurek, R., Klimowicz-Pawlas, A., 2018. Assessment of the pollution and ecological risk of lead and cadmium in soils. *Environ. Geochem Health* 40, 2325–2342.
- Wu, B., Cheng, G., Jiao, K., Shi, W., Wang, C., Xu, H., 2016. Mycoextraction by *Clitocybe maxima* combined with metal immobilization by biochar and activated carbon in an aged soil. *Sci. Total Environ.* 562, 732–739.
- Wu, X., Ba, Y., Wang, X., Niu, M., Fang, K., 2018. Evolved gas analysis and slow pyrolysis mechanism of bamboo by thermogravimetric analysis, Fourier transform infrared spectroscopy and gas chromatography-mass spectrometry. *Bioresour. Technol.* 266, 407–412.
- Xu, Y., Li, X., Cong, G., Gong, G., Xu, Y., Che, J., Hou, F., Chen, H., Wang, L., 2020. Use of resistant *Rhizoctonia cerealis* strains to control wheat sharp eyespot using organically developed pig manure fertilizer. *Sci. Total Environ.* 726, 138568.
- Xu, Z., Xu, X., Tsang, D.C.W., Cao, X., 2018. Contrasting impacts of pre- and post-application aging of biochar on the immobilization of Cd in contaminated soils. *Environ. Pollut.* 242, 1362–1370.
- Yi, Q., Liang, B., Nan, Q., Wang, H., Zhang, W., Wu, W., 2020. Temporal physicochemical changes and transformation of biochar in a rice paddy: Insights from a 9-year field experiment. *Sci. Total Environ.* 721.
- Yi, Y., Kimball, J.S., Rawlins, M.A., Moghaddam, M., Euskirchen, E.S., 2015. The role of snow cover affecting boreal-arctic soil freeze–thaw and carbon dynamics. *Biogeosciences* 12, 5811–5829.

- Yoshida, H., Sazawa, K., Wada, N., Hata, N., Marumo, K., Fukushima, M., Kuramitz, H., 2018. Changes in the chemical composition of soil organic matter including water-soluble component during incubation: A case study of coniferous and broadleaf forest soils. *Catena* 171, 22–28.
- Zeb, A., Li, S., Wu, J., Lian, J., Liu, W., Sun, Y., 2020. Insights into the mechanisms underlying the remediation potential of earthworms in contaminated soil: A critical review of research progress and prospects. *Sci. Total Environ.* 740.
- Zhang, J., Hou, D., Shen, Z., Jin, F., O'Connor, D., Pan, S., Ok, Y.S., Tsang, D.C.W., Bolan, N.S., Alessi, D.S., 2020. Effects of excessive impregnation, magnesium content, and pyrolysis temperature on MgO-coated watermelon rind biochar and its lead removal capacity. *Environ. Res.* 183.
- Zhang, Y., Hou, D., O'Connor, D., Shen, Z., Shi, P., Ok, Y.S., Tsang, D.C.W., Wen, Y., Luo, M., 2019. Lead contamination in Chinese surface soils: Source identification, spatial-temporal distribution and associated health risks. *Crit. Rev. Environ. Sci. Technol.* 49, 1386–1423.
- Zhang, Y., O'Connor, D., Xu, W., Hou, D., 2020b. Blood lead levels among Chinese children: The shifting influence of industry, traffic, and e-waste over three decades. *Environ. Int.* 135.
- Zhao, B., O'Connor, D., Shen, Z., Tsang, D.C., Rinklebe, J., Hou, D., 2020. Sulfur-modified biochar as a soil amendment to stabilize mercury pollution: An accelerated simulation of long-term aging effects. *Environ. Pollut.* 264, 114687.
- Zhao, F.Z., Fan, X.D., Ren, C.J., Zhang, L., Han, X.H., Yang, G.H., Wang, J., Doughty, R., 2018. Changes of the organic carbon content and stability of soil aggregates affected by soil bacterial community after afforestation. *Catena* 171, 622–631.